

## Effect of voltage variation on the performance of carbon electrode supercapacitor cell from saba banana bunch biomass

**Bintang Pamungkas, Awitdrus\***

Department of Physics, Universitas Riau, Pekanbaru 28293, Indonesia

Corresponding author: [awitdrus@lecturer.unri.ac.id](mailto:awitdrus@lecturer.unri.ac.id)

### ABSTRACT

In this study, carbon electrodes for supercapacitors were successfully fabricated using saba banana bunch as a biomass precursor. The electrode preparation process comprised multiple stages, including pre-carbonization, chemical activation with a 0.5 M KOH solution, carbonization at 700°C, followed by physical activation under CO<sub>2</sub> gas at 800°C for 90 minutes. Physical characterization of the carbon electrodes revealed a significant density reduction of 38.51% post-pyrolysis. Surface morphology analysis indicated a porous structure predominantly consisting of micropores and mesopores. Energy-dispersive X-ray (EDX) spectroscopy confirmed a high carbon content, with a mass percentage of 65.24%. Electrochemical performance was evaluated via cyclic voltammetry (CV) and galvanostatic charge-discharge (GCD) measurements at applied voltages of 0.6, 0.8, and 1.0 V. The carbon electrode sample designated SB-1 exhibited the highest specific capacitance values, reaching 74.47 F/g (CV) and 42.58 F/g (GCD). These results indicate that an operating voltage of 1.0 V yields optimal performance for supercapacitor applications employing banana stem-derived carbon electrodes.

**Keywords:** Banana bunch; biomass; carbon electrode; supercapacitor; voltage

Received 06-08-2025 | Revised 29-08-2025 | Accepted 11-11-2025 | Published 17-11-2025

### INTRODUCTION

The energy crisis is becoming an increasingly pressing global issue, especially in Indonesia, where the demand for electrical energy supply continues to increase. Dependence on coal-fired power plants as the main fuel raises concerns because coal is a non-renewable energy source and less environmentally friendly. To overcome this challenge, innovation of energy storage becomes crucial, one of which is the potential utilization of activated carbon [1].

Supercapacitors are advanced energy storage devices that offer several advantages over conventional batteries and capacitors. They are capable of rapid charge and discharge cycles within seconds to minutes and exhibit an exceptionally long cycle life, enduring up to hundreds of thousands of cycles without significant capacity degradation. This performance notably surpasses that of traditional batteries, which typically sustain only 800 to 1,000 cycles. Moreover,

supercapacitors provide high power output, rendering them particularly suitable for applications such as regenerative braking systems in electric vehicles. They also require minimal maintenance and are free from toxic chemicals, thus presenting a more environmentally friendly and safer alternative to lithium-ion batteries, which carry risks of thermal runaway. In addition, supercapacitors demonstrate high resilience to extreme temperatures and harsh environmental conditions. While their energy storage capacity is generally lower than that of batteries, supercapacitors significantly outperform conventional capacitors due to their electrode designs that maximize surface area. Consequently, supercapacitors have found widespread application in electric vehicles, backup power electronics, and renewable energy systems that demand rapid charging and long operational lifespans, positioning them as a promising solution for future energy storage technologies [2].

Activated carbon is an amorphous material made from carbon-based materials specifically designed to have high adsorption capabilities. Because of this ability, activated carbon is often used as an electrode material. Activated carbon is particularly suitable for this purpose, as it has a very high surface area. Various carbon-rich materials, coal, wood, and agricultural waste such as coconut shells [3], bagasse [4], and palm empty fruit bunches [5] can be used as raw materials for making activated carbon [6].

Voltage greatly affects the results of cyclic voltammetry (CV) and Galvanostatic charge discharge (GCD) on supercapacitor carbon electrodes. In CV testing, a larger voltage range can produce a higher specific capacitance because ions in the electrolyte can move more freely within the electrode pores. Increased voltage also increases current, indicating greater storage capacity, but too high a voltage can also create reactions that damage the electrode. In GCD testing, the maximum voltage affects the length of charge and discharge times. Higher voltage makes the discharge time longer, indicating greater stored energy. However, high voltage also increases the sudden voltage drop (IR drop) due to internal resistance, which can lower efficiency and accelerate electrode breakdown. Therefore, choosing the right working voltage is important to obtain optimal supercapacitor performance and lifespan [7]. This study evaluates the effect of voltage variations of 0.6 V, 0.8 V, and 1.0 V on the performance of supercapacitors utilizing activated carbon derived from kepok banana stalks (SB) as the electrode material. The experimental results indicate that an operating voltage of 1.0 V yields the best performance, with specific capacitance ( $C_{sp}$ ) values obtained from CV and GCD tests measured at 74.47 F/g and 42.58 F/g, respectively.

## MATERIALS AND METHODS

### Materials

The Saba banana (SB) stalks were sourced from traditional market waste in Panam,

Pekanbaru. Potassium hydroxide (KOH) at a concentration of 0.5 M was employed as the chemical activator, while sodium sulfate ( $\text{Na}_2\text{SO}_4$ ) at 1 M concentration served as the electrolyte. An eggshell membrane was utilized as the separator. During the electrochemical testing, the voltage was varied to determine the optimal operating voltage for the supercapacitor.

### Preparation of Activated Carbon

The biomass of saba banana bunches was collected, then cut, cleaned with running water, and dried for seven days. The pre-carbonization process was carried out for 4 hours at a temperature of 200°C. After pre-carbonization, the sample was ground using a 53-micron sieve. The powdered banana bunches were chemically activated using a 0.5 M KOH solution, then dried and pulverized again. Pellet molding was performed using a hydraulic press with a pressure of 7 tons. Carbonization was conducted after the pellets were successfully formed, using  $\text{N}_2$  gas at 700°C, followed by physical activation with  $\text{CO}_2$  gas at 800°C, held for 90 minutes. After the carbonization and physical activation stages, the samples were neutralized and polished to a thickness of 0.2 mm and a diameter of 7 mm. During electrochemical testing, voltage variations were applied to determine their effect on the performance of the supercapacitor cells. In this study, three voltage variations were used: 0.6 V (SB-0.6), 0.8 V (SB-0.8), and 1 V (SB-1).

## CHARACTERIZATION

### Density

Density is a measure that shows the ratio between the mass of an materials and its volume. The density equation (Equation 1) is calculated by dividing the total mass of the object by its total volume. The result shows how tightly the material is packed in the space it occupies. density describes how dense an object is. Objects with high density have a large

mass in a small volume. To calculate density, the formula Equation (1) is used [8].

$$\rho = \frac{m}{v} \quad (1)$$

where,  $m$  (g) is the mass, and  $v$  (cm<sup>3</sup>) is the volume of the sample.

## Surface Morphology

The surface morphology of carbon electrode was tested by SEM method. This SEM characterization uses a 6510 (LA) tool with a magnification of 1000 times for the electrode surface measured on the same section for all variations. The results of SEM measurements are micro images of activated carbon electrodes, in which the shape and size of the pores can be observed [9]. The constituent element content of carbon electrodes can be determined by testing using the EDX method. This EDX measurement uses the supra 55VP tool. The principle of elemental analysis of carbon electrodes is by detecting X-rays emitted in the target material. The results of this EDX measurement can be in the form of elemental content of activated carbon electrodes. Elemental analysis in the EDX test is carried out by comparing the ratio of the X-ray intensity of the element contained in the sample with the same element from the standard sample [10].

## Electrochemical Analysis

The electrochemical properties of banana bunch carbon electrodes were evaluated through Cyclic voltammetry (CV) and Galvanostatic charge discharge (GCD) techniques. CV measurements used a potential of 0.6, 0.8, 1 V with a scan rate of 1mV/s. Furthermore, the specific capacitance was calculated using Equations (2) and (3).

$$C_{sp, CV} = \frac{(I_c - I_d)}{s \times m} \quad (2)$$

$$C_{sp, GCD} = \frac{2 I_c \Delta t}{m \cdot \Delta V} \quad (3)$$

where,  $C_{sp}$  is the specific capacitance (F/g),  $I_c$  is the charge current,  $I_d$  is the discharge current (A),  $s$  is the scan rate (mV/s), and  $m$  is the electrode mass (g).

Measurement of electrochemical properties using the GCD method at a current density of 1 A/g. At a voltage between 0.6, 0.8, 1 V with a constant current density of 1 A/g. Furthermore, the specific capacitance value was evaluated using Equation (2), where  $C_{sp}$  is the specific capacitance,  $I$  is the current,  $\Delta t$  is the discharge time,  $m$  is the working mass,  $\Delta V$  is the potential window. Furthermore, the in-depth analysis of banana bunch carbon electrodes for supercapacitor energy storage applications was reviewed through the relationship between energy density and power density calculated using Equations (4) and (5) [11].

$$E_{sp} = \frac{C_{sp} \times \Delta V^2}{7.2} \quad (4)$$

$$P_{sp} = \frac{3600 \times E_{sp}}{\Delta t} \quad (5)$$

## RESULTS AND DISCUSSION

### Density

Figure 1 shows a comparison the graph illustrates the percentage shrinkage of four physical parameters mass, diameter, thickness, and density measured before and after a specific treatment. The mass shrinkage increased from 2.02% before treatment to 7.3% after, indicating a notable loss of material during the process. Diameter shrinkage also rose significantly from 18.94% to 23.77%, demonstrating substantial lateral dimensional changes as a result of the treatment. Thickness showed a smaller increase in shrinkage from 2.23% to 3.09%, yet it still reflects the treatment's effect on the material's thickness dimension. Additionally, density shrinkage increased from 18.94% to 23.77%, which may

indicate changes in the microstructure and porosity of the material post-treatment. Overall, the treatment caused an increase in shrinkage across all physical parameters, with the most prominent changes observed in diameter and density, signifying significant alterations in the material's morphology and characteristics. These findings are critical for understanding the impact of the process on the physical properties of the material and can serve as a reference for process optimization to minimize undesired shrinkage effects.

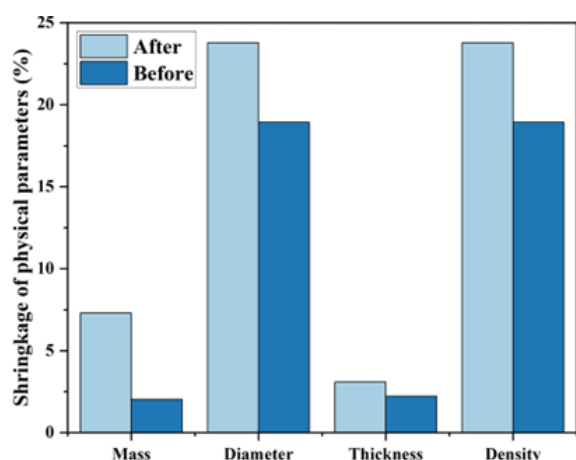


**Figure 1.** Electrode density before and after pyrolysis process.

The significant difference between the before and after conditions shows that the treatment process has a direct effect on the physical properties of the material, which can have an impact on its application performance, for example in supercapacitor electrodes or ceramic materials. Mass shrinkage and density changes can also indicate increased porosity or changes in crystalline structure. Understanding these changes is therefore important in the development of functional materials with desirable physical properties.

### Surface Morphology

The preparation of activated carbon electrodes commenced with chemical activation using a 0.5 M potassium hydroxide (KOH) solution. This step involved chemical reactions that selectively etched the carbon framework derived from the precursor material, thereby

facilitating the formation and enlargement of micropores as well as the generation of new pore structures, which are critical for increasing the electrode's specific surface area. Chemical activation effectively augmented the pore distribution across micro-, meso-, and macropores, thereby enhancing the material's capacity for energy storage.

Subsequently, the chemically activated sample was subjected to carbonization at elevated temperatures to remove volatile constituents and promote the development of a thermally and mechanically stable carbon matrix. This carbonization process also contributed to a partial increase in the crystallinity of the carbon material and established a compact, robust carbon framework, which serves as the structural basis for subsequent pore development. Following carbonization, a physical activation step was implemented using carbon dioxide (CO<sub>2</sub>) gas under controlled thermal conditions. This stage aimed to further develop the pore network by enlarging pore size and improving connectivity, thereby generating an electrode morphology characterized by increased heterogeneity and significantly enhanced surface area. Collectively, the sequence of chemical activation, carbonization, and physical activation synergistically yielded activated carbon materials exhibiting superior porosity and thermal stability, thereby optimizing the electrochemical performance of supercapacitors through improved energy storage capacity and rapid charge-discharge kinetics.

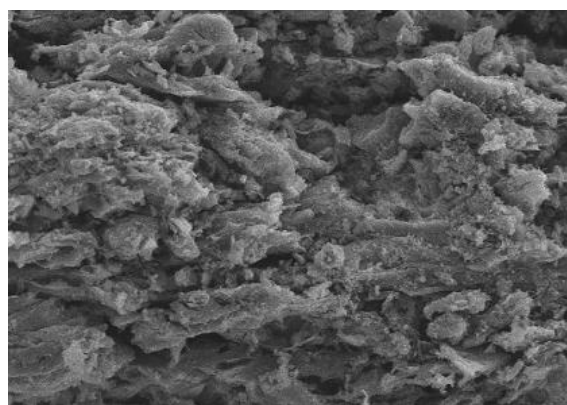


**Figure 2.** Surface morphology of banana bunch carbon electrode 1000x magnification.

Analysis of the elements contained in activated carbon electrodes is essential for understanding the chemical characteristics and performance of these electrodes in supercapacitors. The composition of the main elements and the function of functional groups on the carbon surface affect the stability of the material and its energy storage capacity. An element with relatively low mass compared to carbon consists primarily of nitrogen and oxygen. Nitrogen in banana bunches originates from proteins, amino acids, and other organic nitrogen compounds present in the biomass, while oxygen is derived from functional groups such as hydroxyl, carbonyl, and carboxylate found in cellulose, hemicellulose, and lignin. During carbonization and physical activation, some oxygen-containing groups are released as

gases (CO and CO<sub>2</sub>), whereas others remain on the carbon surface, influencing surface chemistry by enhancing material stability and increasing specific capacitance. The carbon content, sourced from the natural compounds in banana bunches, typically increases during chemical activation and physical activation processes using CO<sub>2</sub> gas, contributing to the development of a robust carbon matrix favorable for energy storage applications.

### Electrochemical Analysis

Cyclic voltammetry (CV) measurements were conducted at various voltage ranges to investigate the electrochemical performance of activated carbon supercapacitors derived from saba banana stalks.

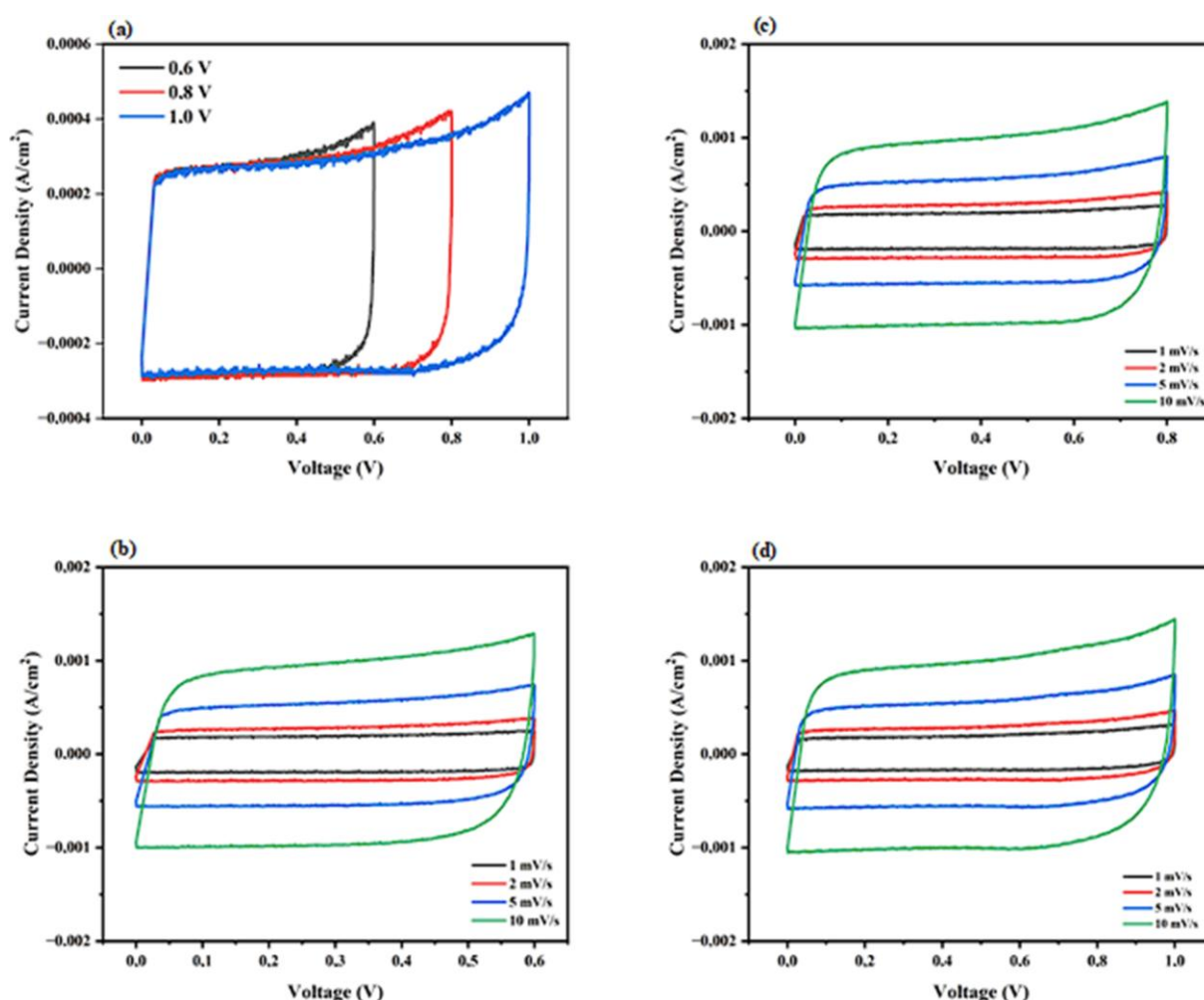


**Figure 3.** CV curve of (a), various voltage 1 mV/s, (b) 0.6 V, (c) 0.8 V, (d) 1.0 V at various scan rate.

At a slow scan rate of 1 mV/s, the CV curve exhibited a nearly rectangular shape with symmetrical current responses, indicative of ideal electric double-layer capacitance (EDLC) behavior and minimal resistive or faradaic contributions. This slow scan rate allowed adequate ion diffusion into the porous electrode structure, providing a reliable estimation of the intrinsic electrochemical capacitance.

Further CV tests were performed under different operating voltages of 0.6 V (SB-0.6), 0.8 V (SB-0.8), and 1.0 V (SB-1.0) to determine the influence of voltage variation on capacitance and electrode stability. At 0.6 V, the CV curve maintained a symmetrical and quasi-rectangular profile, reflecting a dominant capacitive energy storage mechanism with

negligible pseudocapacitive effects. The specific capacitance ( $C_{sp}$ ) calculated from this curve was 67.75 F/g, indicating moderate charge storage capability constrained by the relatively low operating voltage.

Increasing the voltage window to 0.8 V (SB-0.8) resulted in an expanded CV curve area, which corresponds to enhanced charge storage capacity. The specific capacitance increased to 72.03 F/g, demonstrating the positive impact of a wider voltage range on ion adsorption and charge accumulation within the porous carbon matrix. The preservation of CV curve symmetry suggests that the electrochemical processes remained primarily capacitive, with minimal degradation or side reactions evident at this voltage.

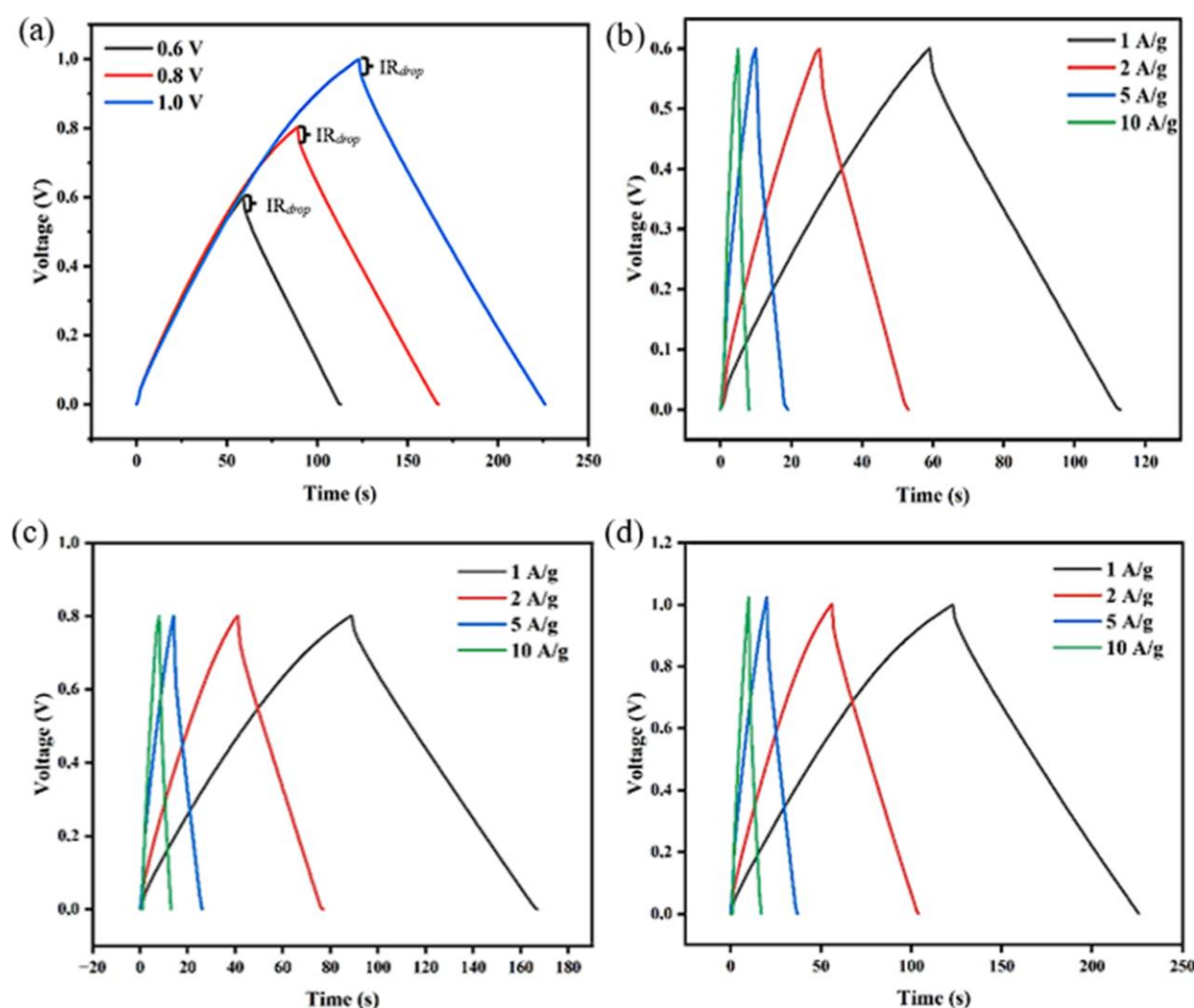


**Figure 4.** GCD of (a) various voltage 1 A/g, (b) 0.6 V, (c) 0.8 V, (d) 1.0 V at various current density.



At the highest tested voltage of 1.0 V (SB-1.0), the CV curve exhibited the largest enclosed area, signifying the highest specific capacitance of 74.47 F/g among all samples. The rectangular shape of the curve was largely maintained, indicating low internal resistance and electrochemical stability, even at this increased voltage. The elevated voltage enhanced the energy storage capability by increasing the potential window. Despite the promising increase in performance, conductive stability and electrolyte limitations at voltages approaching 1.0 V must be carefully considered to prevent long-term degradation. In summary, the observed trend of increasing specific capacitance from 67.75 F/g at 0.6 V, to 72.03 F/g at 0.8 V, and finally 74.47 F/g at 1.0 V demonstrates that operating voltage plays a critical role in optimizing supercapacitor performance. The consistently symmetrical CV curves across the voltage ranges confirm the dominant electric double-layer capacitance mechanism with slight contributions from pseudocapacitance. The optimal operational voltage of 1.0 V balances maximal energy storage with electrode stability, suggesting potential for practical application in energy storage systems based on biomass-derived activated carbon electrodes.

Figure 4 shows the galvanostatic charge-discharge (GCD) curves at three different operating voltage intervals: 0.6 V (SB-0.6), 0.8 V (SB-0.8), and 1.0 V (SB-1.0). The GCD profiles exhibit nearly symmetrical triangular shapes, characteristic of an electric double-layer capacitance (EDLC) energy storage mechanism. At the beginning of charging, the voltage increases linearly until it reaches the peak voltage, followed by a similarly linear voltage drop during discharge. The symmetry and linearity reflect the electrode's low internal resistance and the efficient reversibility of the electrochemical process, indicating a stable activated carbon material.

The GCD curve for SB-0.6 shows an almost perfect triangular shape with good symmetry across different current densities (1, 2, 5, and 10 A/g). At low current (1 A/g), the electrode

demonstrates the longest charge and discharge times, indicating maximal energy storage capacity due to optimal ion diffusion into all pores of the activated carbon. As current increases, the charge-discharge time shortens due to limitations in ion transfer rate and internal resistance, but the curve shape remains symmetrical, indicating a reversible and stable electrochemical process. The  $IR_{\text{drop}}$  in this condition is very low, only 0.01  $\Omega$ , showing minimal internal resistance and efficient charge transfer.

In SB-0.8, the GCD curves also exhibit ideal and nearly symmetrical triangular shapes across all current variations. Compared to SB-0.6, the charge-discharge times at the same currents are slightly longer, indicating improved energy storage capacity due to the higher operating voltage. The IR drop increases slightly to 0.04  $\Omega$  but remains low and does not affect process efficiency. Although discharge time decreases as current increases, electrochemical stability is maintained, indicating the electrode can sustain good performance even at high current densities.

The SB-1.0 GCD curves show similar characteristics to SB-0.8, maintaining ideal and symmetrical triangular shapes across all current densities. The charge-discharge times at the same current tend to be the longest among the three samples, correlating with the highest specific capacitance (42.58 F/g) and specific energy (5.91 Wh/kg). The IR drop remains the same as SB-0.8 at 0.04  $\Omega$ , indicating good stability even at the maximum voltage. The reduction in discharge time at the highest current is still present but not significant, so the electrode maintains reversible efficiency and electrochemical stability under extreme voltage and current conditions.

**Table 1.** Calculation results of  $C_{\text{sp}}$ ,  $E_{\text{sp}}$ ,  $P_{\text{sp}}$ , and  $IR_{\text{drop}}$  values with a current density of 1 A/g.

Voltage (V)	$C_{\text{sp}}$ (F/g)	$IR_{\text{drop}}$ ( $\Omega$ )	$E_{\text{sp}}$ (Wh/kg)	$P_{\text{sp}}$ (W/kg)
SB-0.6	37.78	0.01	5.24	356.50
SB-0.8	40.41	0.04	5.61	262.46
SB-1.0	42.58	0.04	5.91	208.76

Specific capacitance ( $C_{sp}$ ) increases from 37.78 F/g (SB-0.6), 40.41 F/g (SB-0.8), to 42.58 F/g (SB-1.0). This upward trend aligns with the widening of the operating voltage window, allowing for greater charge storage and release capacity by the electrode. The IRdrop remains low, at 0.01  $\Omega$  for SB-0.6 and 0.04  $\Omega$  for SB-0.8 and SB-1.0, indicating minimal internal resistance and good contact between the electrode and current collector, thus maintaining efficient charge transfer.

Specific energy ( $E_{sp}$ ) also increases with voltage, from 5.24 Wh/kg at SB-0.6 to 5.61 Wh/kg at SB-0.8 and 5.91 Wh/kg at SB-1.0, indicating the electrode's ability to store more energy at higher voltages. Specific power ( $P_{sp}$ ) decreases from 356.50 W/kg (SB-0.6) to 262.46 W/kg (SB-0.8) and 208.76 W/kg (SB-1.0). This decline is closely related to increased internal resistance at higher operating voltages, which limits the rate of energy delivery.

Overall, the figures and table above confirm that expanding the operating voltage window up to 1.0 V significantly improves specific capacitance and specific energy while maintaining a low IR drop. This makes activated carbon electrodes from saba banana stalks promising candidates for supercapacitor applications. However, the decrease in specific power at higher voltages warrants further optimization to balance power output, stability, and long-term energy capacity.

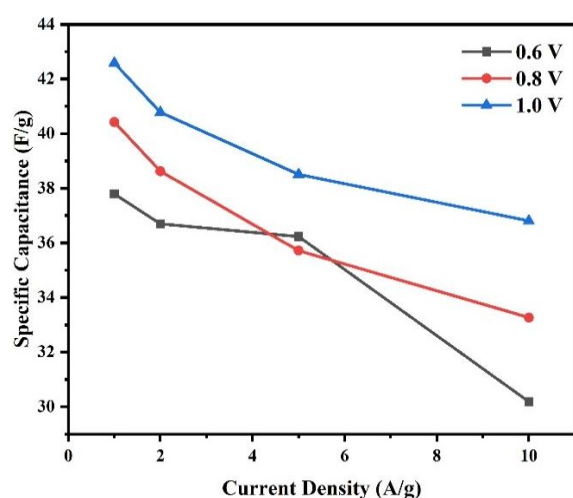


**Figure 5.** Variation of specific capacitance with current density for voltage variation.

Figure 5 shows the relationship between current density (A/g) and specific capacitance (F/g) at three voltages: 0.6 V, 0.8 V, and 1.0 V. As current density increases, specific capacitance decreases due to limited ion diffusion at higher currents. The highest capacitance occurs at 1.0 V across all current densities. At 1 A/g, capacitances are 37.78 F/g (0.6 V), 40.41 F/g (0.8 V), and 42.58 F/g (1.0 V). When current density rises to 10 A/g, capacitance drops significantly for all voltages. This suggests that optimal electrode performance for supercapacitors is achieved at high voltage and low current density.

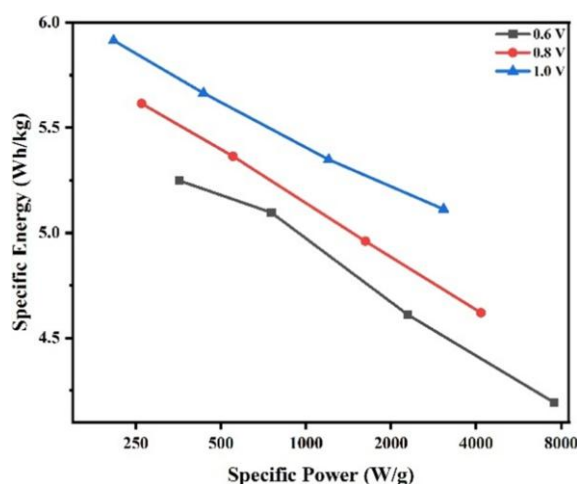


**Figure 6.** Ragone plot of voltage variation.

Figure 6 shows the ragone plot of each voltage variation. It can be seen that the variation with the highest specific power and specific energy is the variation with a voltage of 1.0 V. This shows that the best performing carbon electrode is the electrode with a voltage of 1.0 V.

## CONCLUSION

The study successfully fabricated activated carbon electrodes derived from saba banana stalk biomass through a multi-step process involving chemical activation, carbonization, and physical activation. Physical characterization confirmed a porous carbon structure with dominant micro- and mesopores, accompanied by a significant density reduction,



which favors electrolyte ion adsorption and charge storage.

Electrochemical tests revealed that operating voltage critically affects the performance of the supercapacitor cells. Cyclic voltammetry (CV) showed increasing specific capacitance values of 67.75 F/g, 72.03 F/g, and 74.47 F/g when operating voltages were increased from 0.6 V to 1.0 V, demonstrating enhanced charge storage due to the expanded potential window. Similarly, galvanostatic charge-discharge (GCD) analyses confirmed high reversibility and low internal resistance ( $IR_{\text{drop}}$ ), with the highest specific capacitance of 42.58 F/g and specific energy of 5.91 Wh/kg obtained at 1.0 V and a current density of 1 A/g.

The relationship between current density and specific capacitance showed the expected decrease in capacitance with increasing current density (from 1 to 10 A/g), attributed to limitations in ion diffusion at higher currents. Nevertheless, the electrodes maintained stable charge-discharge behavior across all tested voltages and current densities. The Ragone plot analysis further highlighted the superiority of the 1.0 V operating condition, providing the best balance between specific power and specific energy.

In conclusion, the optimal operating condition for activated carbon electrodes derived from saba banana stalk biomass is an operating voltage of 1.0 V at low current density, where maximum energy storage capacity and electrode stability are realized. These findings support the viability of biomass-derived activated carbon as a sustainable, effective electrode material for supercapacitor applications. Future research should focus on improving power performance and cycling stability to extend practical applicability.

## REFERENCES

- Putri, H., & Farma, R. (2021). Pembuatan dan karakterisasi elektroda karbon aktif dari biomassa pelepah aren dengan persentase KOH. *Komunikasi Fisika Indonesia*, **18**(1), 75.
- Farma, R., Tania, Y., & Apriyani, I. (2023). Conversion of hazelnut seed shell biomass into porous activated carbon with KOH and CO<sub>2</sub> activation for supercapacitors. *Materials Today: Proceedings*, **87**, 51–56.
- Malis, E., Ridho, R., Ayun, Q., Susanti, R. E., Syahputra, D. P. B. (2023). Studi perbandingan sifat elektroda superkapasitor dari arang aktif tempurung kelapa Banyuwangi dengan activator asam dan basa. *Jurnal Crystal: Publikasi Penelitian Kimia dan Terapannya*, **5**(2), 38–45.
- Taer, E., Iwantono, I., Manik S. T., Yulita, M., Taslim, R., & Dahlan, D. (2023). Karbon aktif monolit dari ampas tebu sebagai elektroda superkapasitor: tinjauan siklik voltammetri. *Seminar Nasional Fisika Universitas Andalas (SNFUA)*, **25**(1), 978–979.
- Nofriyanti, W., & Awitdrus, A. (2024). Utilization of young coconut fiber activated carbon with pre-carbonization variations as a supercapacitor electrode. *Indonesian Physics Communication*, **21**(2), 127–130.
- Cahyani, R. F., Nasution, N., & Lubis, R. Y. (2025). Karakterisasi dan kapasitansi elektroda karbon aktif tempurung kemiri dengan variasi aktivator asam fosfat (H<sub>3</sub>PO<sub>4</sub>). *Jurnal Rekayasa Material, Manufaktur dan Energi*, **8**(1), 32–39.
- Siburian, D. H., Rossi, M., & Abrar, A. (2023). Pengaruh variasi massa gliserol pada gel elektrolit untuk aplikasi superkapasitor. *eProceedings of Engineering*, **10**(1), 106–113.
- Utama, K. M., Warji, W., Rahmawati, W., & Suharyatun, S. (2023). Pemanfaatan limbah plastik polyethylene terephthalate (PET) dan batok kelapa sebagai bahan baku paving block. *Jurnal Agricultural Biosystem Engineering*, **2**(2), 262–269.
- Yurdakal, S., Garlisi, C., Özcan, L., Bellardita, M., & Palmisano, G. (2019). (Photo) catalyst characterization techniques: adsorption isotherms and BET,

- SEM, FTIR, UV–Vis, photoluminescence, and electrochemical characterizations. *Heterogeneous Photocatalysis*, 87–152.
10. Shah, F. A., Ruscsák, K., & Palmquist, A. (2019). 50 years of scanning electron microscopy of bone—a comprehensive overview of the important discoveries made and insights gained into bone material properties in health, disease, and taphonomy. *Bone Research*, **7**(1), 15.
11. Simanjuntak, A. C., & Awitdrus, A. (2022). Karakterisasi sifat elektrokimia elektroda karbon aktif berbasis limbah sabut kelapa muda menggunakan separator membran kulit telur ayam. *Indonesian Physics Communication*, **19**(1), 31–34.



This article uses a license  
[Creative Commons Attribution  
4.0 International License](https://creativecommons.org/licenses/by-nc/4.0/)